JOURNAL OF MATERIALS SCIENCE **40** (2005) 711–717

Microstructure and high-temperature strength of $Al_2O_3/Er_3Al_5O_{12}/ZrO_2$ ternary melt growth composite

Y. WAKU*, S. SAKATA**, A. MITANI**, K. SHIMIZU**, A. OHTSUKA
Japan Ultra-High Temperature Materials Research Institute, Ube City, Yamaguchi, 755-0001 Japan
E-mail: hpgtwaku@violin.ocn.ne.jp

M. HASEBE
Department of Materials Science and Engineering, Kyushu Institute of Technology, Sensui-cho, Tobata-ku, Kitakyushu, 804-8650 Japan

A new $Al_2O_3/Er_3Al_5O_{12}$(EAG)/ZrO_2 ternary MGC (Melt Growth Composite) with a novel microstructure has been fabricated by unidirectional solidification. This ternary MGC has a microstructure consisting of continuous networks of single-crystal Al_2O_3, single-crystal EAG and fine cubic-ZrO_2 phases without grain boundaries. The ternary MGC has also characteristic dimensions of the microstructure of around 2–4 μm for EAG phases, around 2–4 μm for Al_2O_3 phases reinforced with around 0.4–0.8 μm cubic-ZrO_2 phases. No amorphous phases are formed at interfaces between phases in the ternary MGC. The ternary MGC's flexural strength at 1873 K is approximately 700 MPa, more than twice the 330 MPa of the Al_2O_3/EAG binary MGC. The fracture manner of the Al_2O_3/EAG/ZrO_2 ternary MGC at 1873 K shows the same intergranular fracture as the Al_2O_3/EAG binary MGC, but is significantly different from the transgranular fracture of the sintered ceramic.

1. Introduction

In the advanced gas turbine field, studies all over the world are seeking to develop ultra-high-temperature structural materials that will improve thermal efficiency in aircraft engines and other high-efficiency gas turbines. So far research is being vigorously pursued into the development of very high temperature structural materials that remain stable under use for prolonged periods in an oxidizing atmosphere at very high temperatures. Ceramics and ceramic-matrix-composites hold promise as structural materials with excellent heat resistance, oxidation resistance, and abrasion resistance and are therefore being examined and developed on a global scale.

As a candidate for a high-temperature structural material, it has been reported that a unidirectionally solidified Al_2O_3/YAG eutectic composite has superior flexural strength, thermal stability and creep resistance at high temperatures [1–3]. As a different eutectic ceramic oxide system, superior mechanical properties at high temperatures of rods with small diameters of the $Al_2O_3/ZrO_2(Y_2O_3)$ system have been reported by Sayir *et al.* [4] and Paster *et al.* [5]. In order to find a new possible development of binary oxide eutectic systems, a microstructural study on ternary oxide systems such as ZrO_2-Y_2O_3-Al_2O_3 and MgO-Al_2O_3-ZrO_2 systems has recently been performed [6, 7]. A lot of this research has principally been focused on the stabilization of ZrO_2 phases with the addition of an Y element [4, 8, 9]. The relation between microstructures and high temperature characteristics has seldom been reported.

Waku *et al.* [10, 11] have recently developed unidirectionally solidified $Al_2O_3/Y_3Al_5O_{12}$ (YAG)/ZrO_2 ternary eutectic composites, termed Melt Growth Composites (MGCs). The ternary MGC has a unique microstructure, which consists of single-crystal Al_2O_3, single-crystal YAG and fine cubic-ZrO_2. This ternary MGC, therefore, displayed superior high-temperature strength characteristics. On the other hand, Nakagawa and Waku *et al.* have developed unidirectionally solidified $Al_2O_3/Er_3Al_5O_{12}$ (EAG) binary MGC [12–14]. The composite is thermally stable and its strength at room temperature can be maintained up to 2073 K. In addition, the compression creep strength at 1873 K and a strain rate of 10^{-4} s^{-1} is approximately 7 times higher than that of sintered composites with the same composition, and the material shows neither weight gain nor grain growth even when heated at 1973 K in an air atmosphere for 1000 h [14]. However, the flexural strength and room temperature fracture toughness of this binary

Present address: HPGT Research Association, Ube City, Yamaguchi, 755-0001 Japan.
**Present address*: Ube Research Laboratory, UBE Industries, LTD., Ube City, Yamaguchi, 755-8633 Japan.

MGC are low. To increase the high temperature flexural strength and room temperature fracture toughness of an Al_2O_3/EAG binary MGC, we have now attempted to fabricate an Al_2O_3/EAG/ZrO_2 ternary MGC reinforced with a ZrO_2 phase by controlling the microstructure using a eutectic reaction of the Al_2O_3-Er_2O_3-ZrO_2 ternary system. In this paper we report on microstructure and high-temperature strength and room temperature fracture toughness of an Al_2O_3/EAG/ZrO_2 ternary MGC compared with an Al_2O_3/EAG binary MGC.

2. Experimental

Commercially available Al_2O_3 powder (AKP-30, Sumitimo Chemical Co., Ltd., Tokyo, Japan), Er_2O_3 powder (Er_2O_3-RU, submicron-type, Shin-etsu Chemical Co., Ltd., Tokyo, Japan) and ZrO_2 powder (TZ-O, Tosoh Co., Ltd., Tokyo, Japan) were mixed to mole ratios of $Al_2O_3/Er_2O_3 = 81/19$ and $Al_2O_3/Er_2O_3/ZrO_2 = 68.4/16.1/15.5$, 67.2/15.8/17.0, 65.9/15.5/18.6 and 64.7/15.2/20.1, and wet ball milling using ethanol was carried out to obtain homogeneous mixed powders. The melting experiments of these mixed powders were performed in the Mo crucible heated by high-frequency induction heating under a pressure of 10^{-5} mmHg of argon, and then, after holding for 30 min at 2173 K, unidirectional solidification was carried out by lowering the Mo crucible at a speed of 5 mm h^{-1} for the binary MGC and 30 mm h^{-1} for the ternary MGC in the same argon atmosphere. For accurate control of crystal growth, a mini-crucible (2 mm in diameter and 17 mm in length) for growing a suitable seed crystal was set at the bottom of the main crucible.

Three-point flexural tests were carried out by using specimens of dimensions of $3 \times 4 \times 36$ mm^3 having the long axis parallel to the solidification direction. The equipment used in this study was a high-temperature uniaxial tension, compression and bending test system (a modified creep and fatigue machine, Instron type 8562). Flexural tests were conducted in an argon gas atmosphere at a crosshead speed of 0.5 mm min^{-1} at 1873 K for the ternary MGC and at room temperature to 2073 K for the binary MGC. The measurement of fracture toughness was performed according to the ASTM E399-90 [15] at room temperature using the same machine used for flexural tests. The dimensions of single edge-notched specimens were $2 \times 4 \times 25$ mm^3. A notch, 2 mm long, was introduced using a diamond wheel. Fracture toughness was calculated using the following equation:

$$K_{\mathrm{Ic}} = (\mathrm{PS})/(\mathrm{BW}^{3/2}) f(a/w)$$

$$f(a/w) = 3(a/w)^{1/2}[1.99 - (a/w)(1 - a/w) \times (2.15 - 3.97a/w + 2.7a^2/w^2)]/[2(1 + 2a/w)(1 - a/w)^{2/3}]$$

Here, P is the load, S is the span, B is the specimen thickness, W is the specimen width, while a is the notch length.

Structural analyses were undertaken using a Rigaku-Denki RAD-RB type X-ray diffraction apparatus. The transmission electron microscope (TEM) observations of the interface and grain-boundary structure between the phases were conducted using a Japan Electron JEM-2010, electron probe microanalysis (EPMA) were undertaken using a Japan Electron JMX-8621MX.

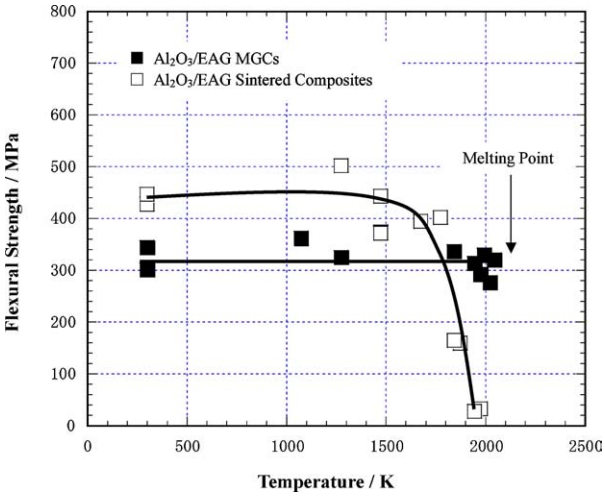

Figure 1 Temperature dependence of flexural strength of an Al_2O_3/EAG MGC compared with Al_2O_3/EAG sintered composites.

3. Results and discussion

3.1. Temperature dependence of flexural strength for Al_2O_3/EAG binary MGC

Fig. 1 shows the temperature dependence of the flexural strength of an Al_2O_3/EAG binary MGC from room temperature to 2073 K in comparison with that of Al_2O_3/EAG sintered composites of the same composition. The binary MGC maintains its room temperature strength up to 2073 K (just below its melting point of about 2130 K), with a flexural strength of approximately 320 MPa. The sintered composite, on the other hand, has the higher flexural strength at room temperature, but its strength falls precipitously above 1773 K [12–14]. The binary MGC has a microstructure in which continuous networks of single-crystal like Al_2O_3 and single-crystal EAG interpenetrate without grain boundaries, colony and porosity [12–14]. In contrast, the sintered composite is a polycrystalline material consisting of grains with random crystal orientation [12–14].

Sintered composites show intergranular fracture at room temperature and at 1673 K, while the binary MGC shows no grain growth up to the very high temperature of 1973 K, and the fracture is transgranular. Moreover, when the test temperature reaches 2073 K, fracture of the interface between Al_2O_3 and EAG phases and mixed fracture of intergranular and transgranular is observed [12–14].

3.2. Al_2O_3/EAG/ZrO_2 ternary eutectic MGC

3.2.1. Computer simulation of a liquidus surface in the Al_2O_3/Er_2O_3/ZrO_2 ternary equilibrium diagram

To obtain thermodynamic parameters necessary to calculate the $Al_2O_3/Er_2O_3/ZrO_2$ ternary equilibrium diagram by a computer, thermodynamic analysis between

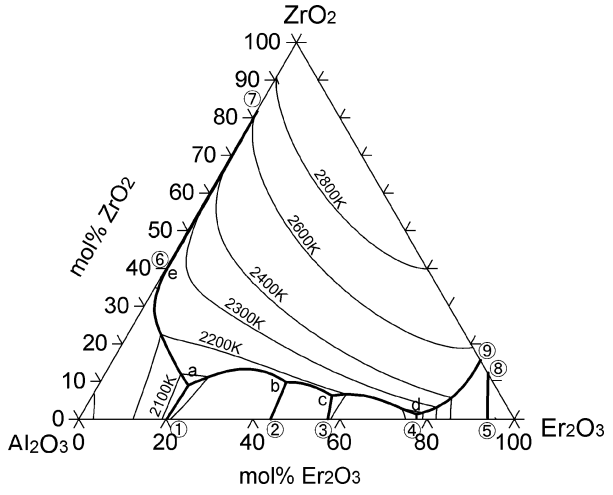

Figure 2 Showing a liquid surface diagram in an $Al_2O_3/Er_2O_3/ZrO_2$ ternary equilibrium system calculated by computer using a CALPHAD method.

experimental and calculated equilibrium diagrams were performed using Al_2O_3/Er_2O_3 binary [16], Al_2O_3/ZrO_2 binary [17] and Er_2O_3/ZrO_2 binary [18] diagrams. The main objective of computer simulation in this study is to obtain a liquidus surface diagram, we therefore neglect equilibrium state treatment between solid phases due to several complex phase transformations in an Er_2O_3/ZrO_2 binary system. Fig. 2 shows a liquidus surface diagram in $Al_2O_3/Er_2O_3/ZrO_2$ ternary equilibrium system simulated by a computer using a CALPHAD method. It is found that there are four ternary eutectic compositions, a, b, c and d in Fig. 2.

In the case of $Al_2O_3/Er_2O_3/ZrO_2 = 70.5/20.5/9.0$ mole ratio ('a' eutectic composition in Fig. 2), no cracks can be observed in the unidirectionally solidified composite. Therefore, this composition system may be produced *in situ* by the unidirectional solidification process, with the composite consisting of Al_2O_3 phase, EAG phase and ZrO_2 phase. Referring to "a" eutectic composition in Fig. 2, several compositional experiments were conducted, increasing the amount of ZrO_2.

3.2.2. Microstructure

The microstructure of the unidirectionally solidified ternary hypoeutectic composite with ZrO_2 less than 18.6 mole ratio consists of a large primary crystal, which is the Al_2O_3/EAG binary eutectic, and a fine Al_2O_3/EAG/ZrO_2 ternary eutectic. The dimensions of the primary crystal are nearly the same as that of an Al_2O_3/EAG binary MGC. The volume of primary crystal decreases with increasing ZrO_2 content.

At a ZrO_2 content equal to 18.6 mole ratio, we can obtain a fine and uniform microstructure consisting of only Al_2O_3/EAG/ZrO_2 ternary eutectic. Fig. 3 shows SEM images of the cross-section perpendicular to the solidification direction of the ternary MGC with a mole ratio of $Al_2O_3/Er_2O_3/ZrO_2 = 65.9/15.5/18.6$ (Fig. 3a and b) in comparison with that of an Al_2O_3/EAG binary MGC with a mole ratio $Al_2O_3/Y_2O_3 = 81/19$ (Fig. 3c). The microstructure of the ternary MGC

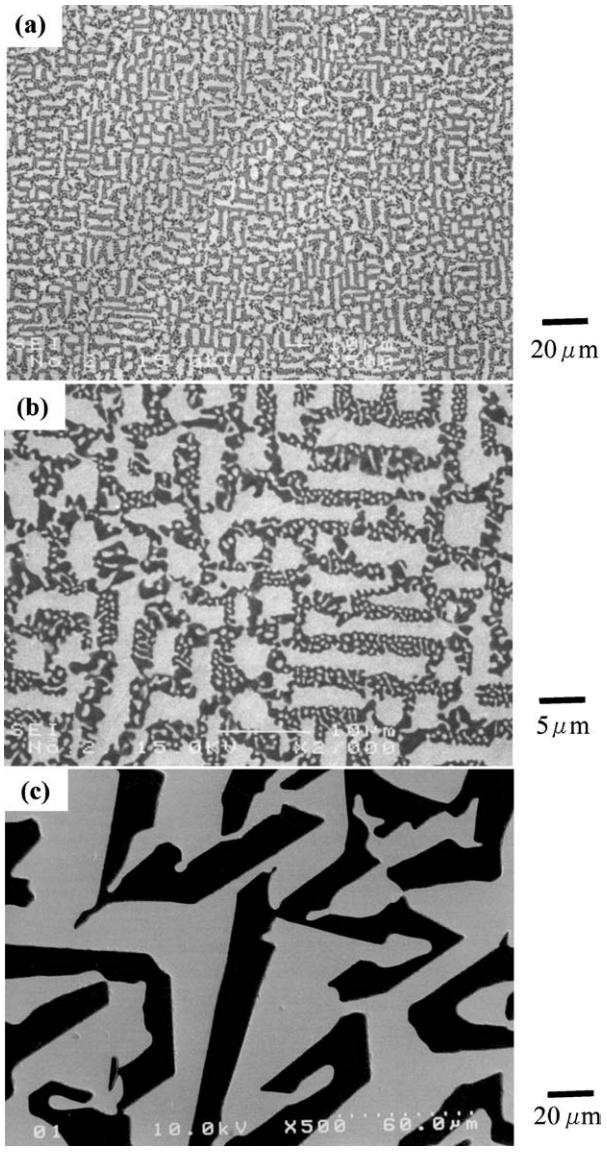

Figure 3 SEM images showing the microstructure of a cross-section perpendicular to the solidification direction of the Al_2O_3/EAG/ZrO_2 ternary MGC. (a) and (b) Al_2O_3/EAG/ZrO_2 ternary MGC. (b) an enlarged image of (a), (c) Al_2O_3/EAG binary MGC.

consists of Al_2O_3, EAG phases and fully stabilized $Zr_{0.8}Er_{0.2}O_{1.9}$ phases with an erbium element for the Al_2O_3/EAG/ZrO_2 ternary MGC, and Al_2O_3 and EAG phases for the Al_2O_3/EAG binary MGC (we describe these $Zr_{0.8}Er_{0.2}O_{1.9}$ phases as cubic-ZrO_2 phases in the following); these were determined from X-ray diffraction patterns. The large gray area like a plate form in the SEM micrograph is the EAG phase, the dark area is the Al_2O_3 phase and fine gray area in the Al_2O_3 phase is the cubic-ZrO_2 phase as shown in Fig. 2b (identified by X-ray diffraction and EPMA analysis). The dimensions of EAG phases in the Al_2O_3/EAG/ZrO_2 ternary MGC are around 2–3 μm (this dimension is defined as the typical length of the short axis of each domain seen in the cross-section perpendicular to the solidification direction) smaller than 1/10, at around 20–30 μm, of the Al_2O_3/EAG binary MGC. Many of the ZrO_2 phases exist at interfaces between Al_2O_3 and EAG phases or in Al_2O_3 phases, and seldom exist in EAG phases. The dimensions of the fine cubic-ZrO_2 are

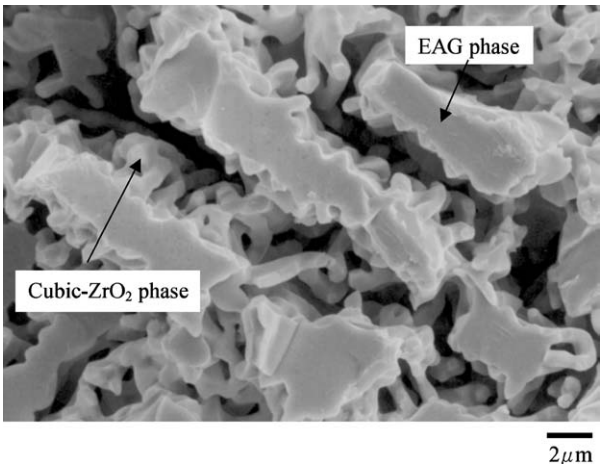

Figure 4 SEM micrograph showing the three-dimensional configuration of single-crystal EAG and ZrO_2 phases in the Al_2O_3/EAG/ZrO_2 ternary MGC.

0.4–0.8 μm. Homogeneous microstructures with no pores or colonies are observed in the unidirectionally solidified binary and ternary system ceramics (Fig. 3a–c).

In the X-ray diffraction pattern for the ternary MGC, diffraction peaks from the (0006) and (00012) plane of the Al_2O_3 phase, from the (400) and (800) plane of the EAG phase and from the (200), (400) and (220) plane of the ZrO_2 phase are observed only from the plane perpendicular to the solidification direction. Consequently, it can be concluded that this ternary MGC consists of ⟨0001⟩ single-crystal Al_2O_3 with a hexagonal structure, ⟨100⟩ single-crystal EAG with a garnet structure and fine ⟨100⟩ and ⟨110⟩ ZrO_2 phases with a cubic structure.

Fig. 4 shows a SEM micrograph which illustrates the three-dimensional configuration of the single-crystal EAG and the ZrO_2 phase in the ternary MGC from which Al_2O_3 phases had been removed by heating in graphite powders at 1923 K for 2 h. The large lump, assembling a plate, in the SEM micrograph is the EAG phase, and the fine rod like material attached to the surface of the EAG phase or between EAG phases is the cubic-ZrO_2 phase as shown in Fig. 4. The configuration of single-crystal EAG and fine cubic-ZrO_2 phases is a three-dimensionally connected porous structure with irregular shape. We therefore conclude that the present ternary MGC has a microstructure consisting of three-dimensionally continuous and complexly entangled single-crystal Al_2O_3, single crystal EAG and fine cubic-ZrO_2 phases. This microstructure was fabricated by controlling accurately crystal growth and the solidification process in the unidirectional solidification. This ternary MGC's room-temperature fracture toughness is approximately 5.2 $MPam^{1/2}$, which is much higher than that of around 3 $MPam^{1/2}$ of the Al_2O_3/EAG binary MGC.

3.2.3. Interface

The existence of amorphous phases at interfaces or grain boundaries generally leads to a reduction in the strength of the material at high temperatures [19, 20]. Fig. 5 shows typical high-resolution TEM images of the interfaces between EAG and cubic-ZrO_2 phases in the Al_2O_3/EAG/ZrO_2 ternary MGC. No amorphous phases are observed at the interfaces between the EAG and cubic-ZrO_2 phases. A similar result was observed at other interfaces between the Al_2O_3 and EAG phases, Al_2O_3 and c-ZrO_2 phases. All the interfaces observed are relatively compatible.

3.2.4. High temperature flexural strength

Fig. 6 shows typical stress-displacement curves of the Al_2O_3/EAG/ZrO_2 ternary MGC obtained from the flexural test at 1873 K. For comparison, a stress-displacement curve for an Al_2O_3/EAG binary MGC [12–14] is also shown. Flexural strength of the Al_2O_3/EAG/ZrO_2 ternary MGC is approximately 700 MPa and appreciably higher than that of the Al_2O_3/EAG binary MGC. The relative fracture energy of the Al_2O_3/EAG/ZrO_2 ternary MGC (which can be inferred from the area under the stress-strain curve) is several times that of the Al_2O_3/YAG binary MGC [12–14].

The change in flexural strength of the unidirectionally solidified Al_2O_3/EAG/ZrO_2 ternary composite at 1873 K with additional amount of ZrO_2 is shown in Fig. 7. The flexural strength of the unidirectionally solidified composite depends substantially on the additional amounts of ZrO_2. When the additional amount of ZrO_2 reaches 18.6 mole ratio, the fine and uniform ternary eutectic microstructure appears (Fig. 3a and b), and the ternary MGC's average flexural strength at 1873 K is approximately 700 MPa, more than twice that, at around 336 MPa, of the Al_2O_3/EAG binary MGC fabricated at a lowering speed of 5 mm h^{-1} of the Mo crucible (Fig. 7).

Fig. 8 shows a SEM image of the fracture surface of a flexural tested specimen at 1873 K for the present ternary MGC. The large region having plate-like form in the SEM image is single-crystal EAG. Among these EAG phases, a single-crystal Al_2O_3 was observed with fine dispersions of cubic-ZrO_2. The fracture surface of Al_2O_3 phases is irregular, showing that cubic ZrO_2 is more resistant to fracture. Seemingly, the fracture mode of the cubic-ZrO_2 in the Al_2O_3 phase is intergranular, however, it is presumed to be a transgranular fracture from the evidence of a continuous network of cubic-ZrO_2 seen in Fig. 4. Single-crystal ZrO_2 readily shows plastic deformation at above 1673 K [21] and a transition temperature from brittle to ductile behavior for single-crystal Al_2O_3 of 1300–1333 K [22]. Therefore, the round shape of fine cubic-ZrO_2 seen on the fracture surface is likely to be due to the fact that single-crystal Al_2O_3 and fine cubic-ZrO_2 deform plastically at 1873 K. The fracture mode of the Al_2O_3/EAG/ZrO_2 ternary MGC at 1873 K is intergranular and completely different from the transgranular fracture of sintered ceramics [12–14].

According to Hillig [23], the strength of brittle materials should decrease proportionally to $T/T_m^{3/2}$, where T_m is the melting temperature. At 0.5 T_m, the strength is around half that at room temperature because

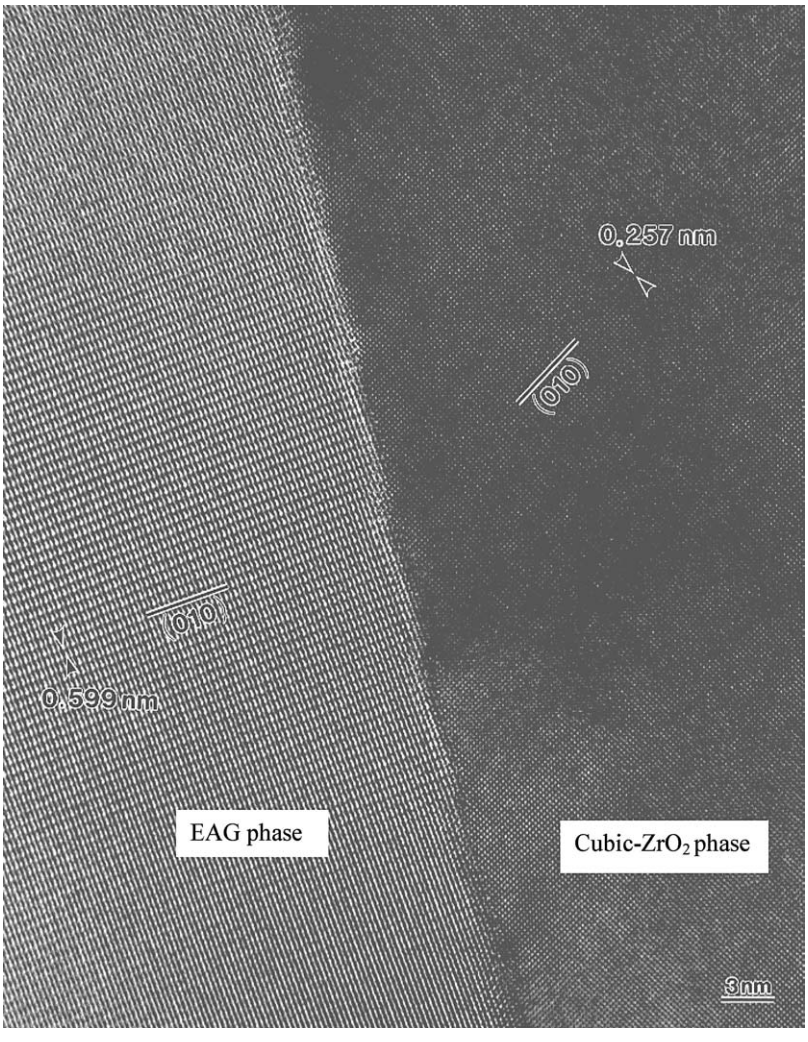

Figure 5 High-resolution TEM images of the interface between EAG and cubic-ZrO_2 phases of the Al_2O_3/EAG/ZrO_2 ternary MGC. The beam directions are [001] Al_2O_3, [001] EAG and [001] ZrO_2.

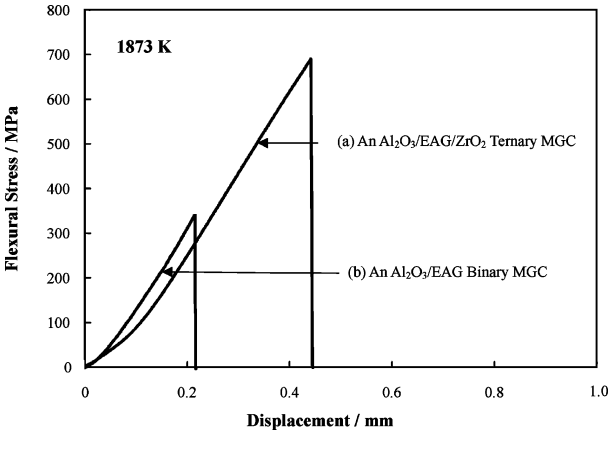

Figure 6 Typical stress-displacement curves in the three-point flexural test at 1873 K of (a) an Al_2O_3/EAG/ZrO_2 MGC compared with (b) an Al_2O_3/EAG binary MGC.

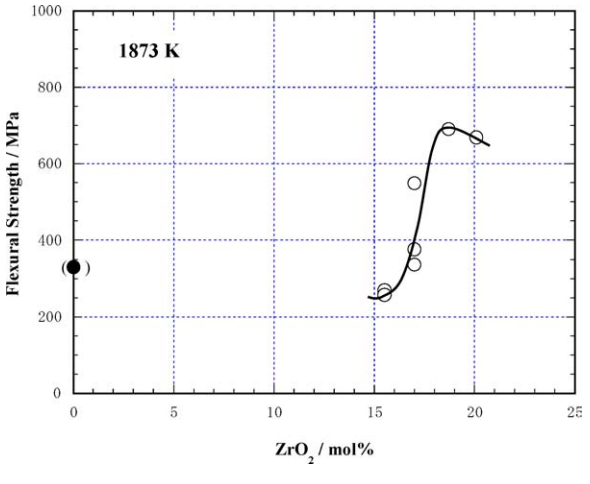

Figure 7 Dependence of flexural strength at 1873 K on the additional amount of ZrO_2 for the Al_2O_3/EAG/ZrO_2 ternary MGC.

at high temperatures, diffusional processes at grain boundaries, which lead to plastic deformation, play a large role. The ternary MGC has a unique microstructure in which single-crystal phases interpenetrate without grain boundaries. The average flexural strength of the Al_2O_3/EAG/ZrO_2 ternary MGC is therefore around 700 MPa at 1873 K and much higher than that (~550 MPa) at 1773 K of an advanced Si_3N_4ceramic recently developed for high temperature structural materials [24].

3.2.5. Stabilization of ZrO_2

Fig. 9 shows X-ray diffraction patterns of the Al_2O_3/EAG/ZrO_2 ternary MGC from room

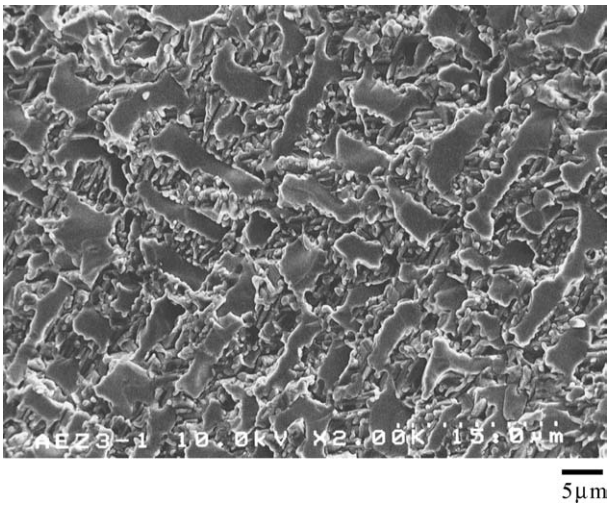

Figure 8 A SEM photograph showing fracture surfaces in flexural tested specimens at 1873 K of the $Al_2O_3/EAG/ZrO_2$ ternary MGC.

temperature to 1773 K compared with the Al_2O_3/ZrO_2 binary MGC without the stabilization element erbium. It is found that the monoclinic-to-tetragonal transformation exists above 1273 K in the Al_2O_3/ZrO_2 binary MGC without the stabilization element erbium (Fig. 9a). However, in the case of the $Al_2O_3/EAG/ZrO_2$ ternary MGC, the monoclinic-to-tetragonal transformation between room temperature and 1773 K does not occur due to the formation of fully stabilized cubic-ZrO_2 phases with an erbium element (Fig. 9b).

4. Conclusions

We conclude that the superior high-temperature strength of $Al_2O_3/EAG/ZrO_2$ ternary MGC over Al_2O_3/EAG binary MGC was obtained by the following means: a new combination of single-crystal Al_2O_3 with a hexagonal structure, single-crystal EAG with a garnet structure and fine ZrO_2 with a cubic structure; a microstructure consisting of three-dimensionally continuous and complexly entangled single-crystal Al_2O_3, single-crystal EAG and fine cubic-ZrO_2; characteristic dimensions of the microstructure of the $Al_2O_3/EAG/ZrO_2$ ternary MGC of around 2–3 μm for EAG phases, around 2–3 μm for Al_2O_3 phases and 0.4–0.8 μm for ZrO_2 phases, finer than that of the ~20–30 μm for the Al_2O_3/EAG binary MGC; and the fact that no amorphous phase is formed at interfaces

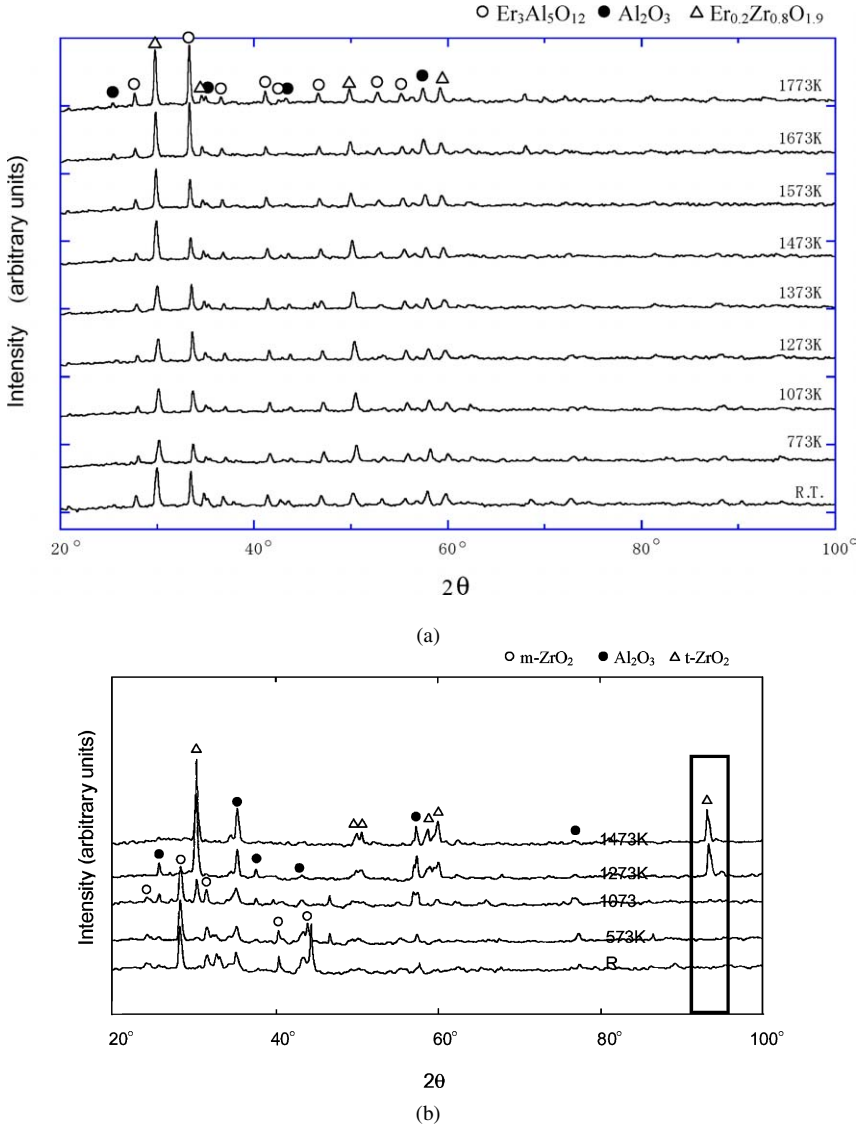

Figure 9 X-ray diffraction patterns of (a) the $Al_2O_3/EAG/ZrO_2$ ternary MGC from room temperature to 1773 K in comparison with (b) the Al_2O_3/ZrO_2 binary MGC.

between the Al_2O_3 and EAG phases, the Al_2O_3 and ZrO_2 phases, the EAG and ZrO_2 phases. It is possible that the two phases are bound together strongly at these interfaces.

Acknowledgments

The authors would like to express their thanks to the New Energy and Industrial Technology Development Organization (NEDO) and the Ministry of Economy, Trade and Industry (METI) for the opportunity to conduct "Research on Technology for MGC Ultra-High-Efficiency Gas-Turbine."

References

1. T. MAH and T. A. PARTHASARATHY, *Ceram. Eng. Sci. Proc.* **11** (1990) 1617.
2. T. A. PARTHASARATHY, T. MAH and L. E. MATSON, *ibid.* **11** (1990) 1628.
3. T. A. PARTHASARATHY, TAI-II MAR and L. E. MATSON, *J. Am. Ceram. Sci.* **76** (1993) 29.
4. A. SAYIR and S. C. FARMER, *Acta Mater.* **48** (2000) 4691.
5. J. Y. PASTOR, P. POZA, J. LLORCA, J. I. PENA, R. I. MERINO and V. M. ORERA, *J. Am. Ceram. Sci.* **83** (2000) 2745.
6. T. A. LOPATO, L. V. NAZARENKO, G. I. GARASIMYUK and A. V. SCHEVCHENKO, *Inorg. Matl.* **26** (1990) 701.
7. J. MCKITTRICK and G. KALONJI, *Mater. Sci. Eng.* **A231** (1997) 90.
8. J. ECHIGOYA, Y. TAKABAYASHI and H. SUTO, *J. Mater. Sci. Letter* **5** (1986) 153.
9. V. A. BORDEIN, M. YU. STAROSTIN and T. N. YALOVETS, *J. Crystal Growth* **104** (1990) 148.
10. Y. WAKU, S. SAKATA, A. MITANI and K. SHIMIZU, *Mat Res Innovat.* **5** (2001) 94.
11. Y. WAKU, S. SAKATA, A. MITANI, K. SHIMIZU, A. OHTSUKA and M. HASEBE, *J. Mater. Sci.* **37** (2002) 2975.
12. N. NAKAGAWA, Y. WAKU and T. WAKAMOTO, *Mater. Manufact. Proc.* **15** (2000) 709.
13. N. NAKAGAWA, Y. WAKU, T. WAKAMOTO, H. OHTSUBO, K. SHIMIZU and Y. KOHTOKU, *J. Jpn. Inst. Metals* **64** (2000) 101.
14. Y. WAKU, N. NAKAGAWA, H. OHTSUBO, A. MITANI and K. SHIMIZU, *J. Mater. Sci.* **36** (2001) 1585.
15. ASTM Standard E399-90, *Annual Book of ASTM Standard* **03.01** (1990) 407.
16. M. Mizuno, *Yogyo Kyokaishi.* **87** (1979) 405.
17. G. R. FISCHER, L. J. McNALLY and R. N. DOMAN, *J. Mater. Sci.* **16** (1981) 3447.
18. A. ROUANET, *Rev. Int. Hautes Temp. Refract.* **8** (1971) 161.
19. D. R. CLARKE, *J. Am. Ceram. Soc.* **62** (1979) 236.
20. J. ECHIGOYA, S. HAYASHI, K. SASAKI and H. SUTO, *J. Jpn Inst. Metals* **48** (1984) 430.
21. K. J. McCLELLAN, H. SAYIR, A. H. HEUER, A. SAYIR, J. S. HAGGERTY and J. SIGALOVSKY, *Ceram. Eng. Sci. Proc* **14** (1993) 651.
22. H. S. KIM and S. ROBERTS, *J. Am. Ceram. Soc.* **77** (1994) 3099.
23. W. B. HILLIG, in Tailoring Multiphase and Composite Ceramics, edited by Richard E. Tressler, Gray L. Messing, Carlo G. Pantano and Robert E. Newnham (Plenum Press, Materials Science Research 1986) Vol. 20, p. 697.
24. M. YOSHIDA, K. TANAKA, T. KUBO, H. TERAZONE and S. TSURUZONE, in Proceedings of the international Gas Turbine & Aeroengine Congress & Exibition, Stockholm (The American Society of Mechanical Engineeers, Sweden, 1998) p. 1.

Received 12 December 2003
and accepted 24 September 2004